Spring 2009

Automatic vessel and telangiectases analysis in dermoscopy skin lesion images

Beibei Cheng

AUTOMATIC VESSEL AND TELANGIECTASES ANALYSIS

IN DERMOSCOPY SKIN LESION IMAGES

By

BEIBEI CHENG

A THESIS

Presented to the Faculty of the Graduate School of the

MISSOURI UNIVERSITY OF SCIENCE AND TECHNOLOGY

In Partial Fulfillment of the Requirements for the Degree

MASTER OF SCIENCE

In

COMPUTER ENGINEERING

2009

Approved by

R. Joe Stanley, Advisor

Randy H. Moss

William V. Stoecker

ABSTRACT

The blood vessels are part of the circulatory system and function to transport blood throughout the body. Vessels have their own features such as distinctive color compared to surrounding skin as well as distinctive curved and/or linear shape. Telangiectases are small dilated blood vessels near the surface of the skin or mucous membranes, measuring between 0.5 and 1 millimeter in diameter. In this research, image analysis techniques are investigated to detect vessels in dermoscopy skin lesion images. Machine vision and neural network methods are explored to discriminate skin lesions containing telangiectases from those containing normal vessels.

A vessels Detection technique is implemented firstly to find the possible vessels in dermatology skin lesion images. In addition, a noise filtering technique is applied, which filters out the "noise" such as hair, bubble and so on, according to their own features. Based on the fact that some of the images are fuzzy, a contrast enhancement technique can be added to increase the contrast. After obtaining the final masked regions containing vessel-like structures, features are computed to facilitate the discrimination of skin lesion with normal vessels from lesions containing telangiectases. The features are mostly about the number, shape and size of telangiectases mask.

Two different artificial neural networks including back-propagation artificial neural networks (BP-ANN) and Particle Swarm Optimization (PSO) as a part of neural network are examined for vessel discrimination on a skin lesion by skin lesion basis. Experiments and results are reported for vessel detection and discrimination. Conclusion and the future scope are shown in the last.

ACKNOWLEDGMENTS

I would like to express my gratitude to my advisor, Dr. R. Joe Stanley, whose expertise, understanding, and patience, added considerably to my graduate experience. I appreciate his vast knowledge and skills in many areas and his assistance in writing this thesis. I would like to thank Dr. William V. Stoecker, who supports me and takes time out from his busy schedule to serve as my external supervisor to help keep me challenge myself.

I thank David Erdos, whose initial work on this project established the platform where I could carry on. I also wish to thank my committee member Dr. Randy H. Moss for his guidance and support.

I would also like to thank my family for the support they provided me through my entire life and in particular, I must acknowledge my mother's love and encouragement that motivated me to keep moving on and overcoming the difficulties. I thank my friend, Soumya, for giving me a chance to share my good and not-so-good times in graduate school.

TABLE OF CONTENTS

LIST OF ILLUSTRATIONS

LIST OF TABLES

1. INTRODUCTION

Telangiectases are widely open (dilated) blood vessels in the outer layer of the skin. They are very common in healthy people and are usually caused by sun damage or aging. When seen on the legs, they do not necessarily indicate a vein disorder, such as varicose veins or underlying deep vein problems. Figure 1.1 presents an example of a dermoscopy skin lesion image with telangiectases present in (a) and a skin lesion image with normal (indistinct) vessels present in (b) (Many lesions have rudimentary vascular structures. The challenge here is to differentiate the short, rather indistinct from the longer, clear vessels of skin cancer). The arrow in Figure 1.1 (a) points to an area with telangiectases present.
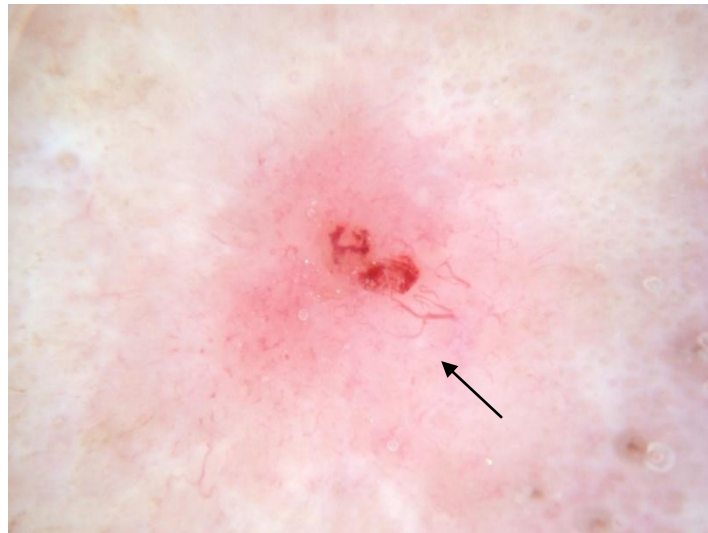
(a) Telangiectases

Figure 1.1: Skin Lesion Example.
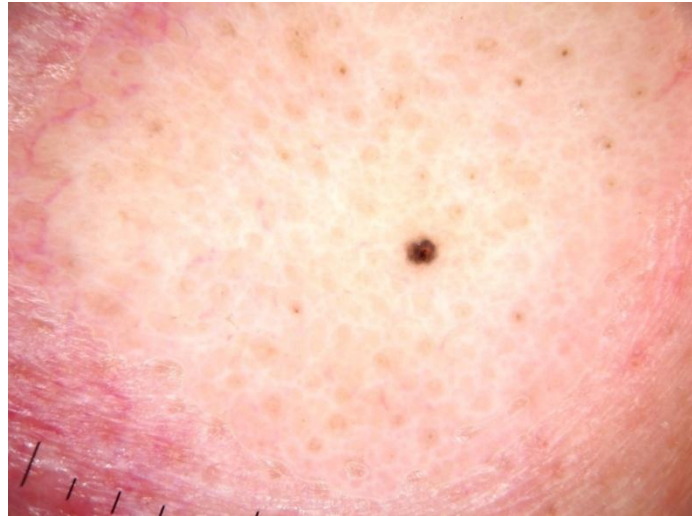
(b) Normal (Indistinct) Vessels

Figure 1.1: Skin Lesion Example. (cont.)

These vessels are observed with a number of diseases, including acne rosacea, birthmarks (eg, port-wine stains), scleroderma, several types of inherited disorders (ataxia-telangiectases, hereditary hemorrhagic telangiectases, xeroderma pigmentosum, and others), or with prolonged use of oral or topical corticosteroids [1]. Therefore, it is very necessary to discriminate Telangiectases as early as possible to avoid any danger. In this research, image analysis techniques are investigated to detect vessels in dermoscopy skin lesion images. Characteristic features of the vessels are examined to foster the discrimination of normal vessels from Telangiectases on a skin lesion by skin lesion basis.

Color and shape features are used for vessel characterization. Color is an important skin lesion feature for detecting vessels. The red, green and blue (RGB) color space is

used to represent colors characteristic of each image. For RGB space, there are eight bits per pixel, providing 256 possible values for each of the components. Thus, there are a total of 256^3 possible colors in this color space. However, there is a problem with detecting vessel based on color, which is that quantifying the colors considered characteristic of vessels is difficult due to variations in lighting and slide processing whether using photography or digital imaging. The use of relative color, in which the average background skin color is subtracted from each lesion pixel, has been proposed as a technique to help compensate for color distortion in the imaging process. This technique equalizes color changes due to different skin types as well as to lighting and image processing techniques [2].

Therefore, the basic approach investigated for detecting vessels is according to the fact that vessel has different color with surrounding skin. The vessels detection technique is implemented firstly to find the possible vessels in dermatology skin lesion images using the red, green and blue color drop between the pixels inside vessel and the surrounding pixels in eight directions, including East, South, West, North, Northwest, Northeast, Southwest and Southeast.

In addition, shape is an important skin lesion feature for discriminating lesions with telangiectasias from others. For example, the area of vessels, the length of vessels and the number of vessels could be generated as the features for data sets. Dermoscopy image sets consisting of skin lesions with and without telangiectases are examined for vessel feature-based discrimination. Two different artificial neural networks, including multi-layer perception back-propagation neural networks (BP-ANN) and Particle Swarm

Optimization (PSO) based neural network are examined for vessel discrimination on a skin lesion by skin lesion basis.

The remaining sections of this thesis include: 1) the vessel detection technique, 2) the image noise filtering technique, 3) the neural network methods for lesion-based vessel discrimination, 4) experiments performed, results and discussion and 5) conclusions and the scope of future research.

2. METHODOLOGY

An overview of the methodology for this research is provided in the flowchart in Figure 2.1. This study uses dermoscopy skin lesion images containing 59 Telangiectases images and 235 competitive benign images as the input sets. Those images are from the following clinics 1)Stoecker & Associates, Rolla, MO (W.V. Stoecker, D. Calcara), 2) Skin and Cancer Associates, Plantation, FL (H.S. Rabinovitz and M. Oliviero), 3) The Dermatology Center, Rolla, MO (J. Malters), 4) Sheard & Drugge PC, Stamford, CT (R. Drugge), and 5) Boone Clinic, Columbia, MO (L.A. Perry). From Figure 2.1, the basic approach for dermoscopy skin lesion analysis is to apply vessel detection and noise filtering techniques to generate an output binary vessel mask. Since a vessel looks redder than the surrounding skin, the vessel detection technique uses color drop from the surrounding pixels to mark the possible vessel pixels. However, other areas such as hair, bubble and so on might still be marked falsely because they may also meet the color drop requirement. The noise filtering technique is used to mitigate these noise sources. Then, image-based features are computed based on the vessel mask. This process is performed for all images in the data set. Image-based vessel discrimination is done for the two classes of skin lesions with telangiectases and without telangiectases.

A training data set of the images is used and the remaining data set of the images is used for the test set. Image-based telangiectases discrimination is performed using different neural network classifiers.

```
┌─────────────────┐      ┌──────────────┐      ┌──────────────┐      ┌─────────────────┐
│ Telang Images & │ ──▶  │ Vessel       │ ──▶  │ Noise Filter │ ──▶  │ Images with     │
│ No-telang       │      │ Detection    │      │ Technique    │      │ Telang Mask     │
│ Images          │      │ Technique    │      │              │      │                 │
└─────────────────┘      └──────────────┘      └──────────────┘      └─────────────────┘
                                                                              │
                                                                              ▼
                                                                      ┌──────────────┐
                                                                      │ Feature      │
                                                                      │ Generation   │
                                                                      └──────────────┘
                                                                              │
                                                                              ▼
┌─────────────────┐      ┌──────────────┐      ┌──────────────┐      ┌─────────────────┐
│ Telang & No-    │ ◀──  │ Neural       │ ◀──  │              │ ◀──  │ Telang Data Set │
│ Telang Image    │      │ Network      │      │              │      │ & No-Telang     │
│ Classification  │      │ Classification│     │              │      │ Data Set        │
└─────────────────┘      └──────────────┘      └──────────────┘      └─────────────────┘
```
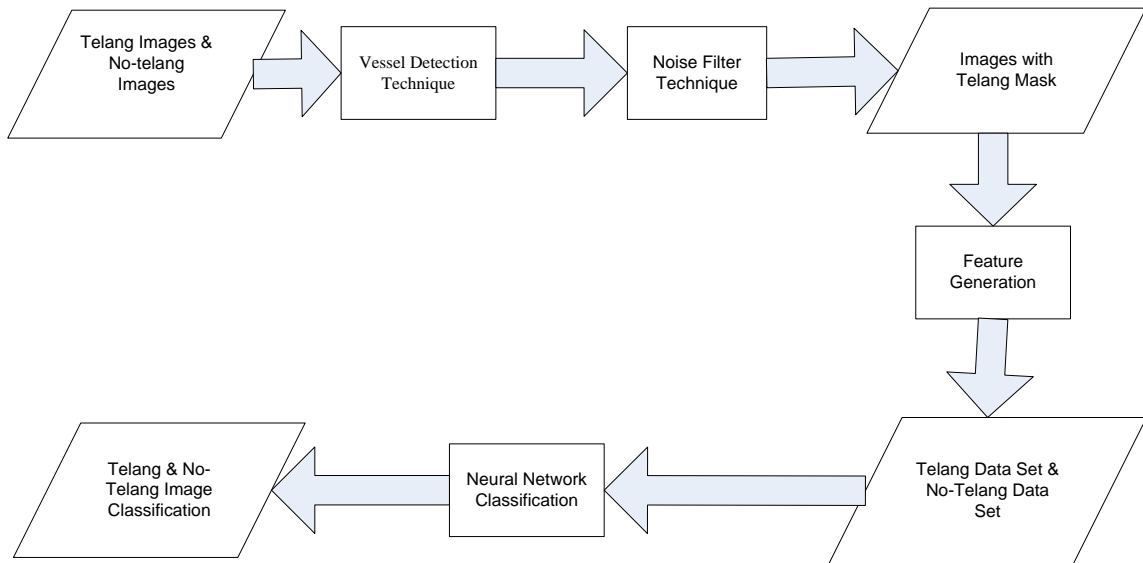
Figure 2.1: Overview of Vessel Detection and Discrimination Process.

2.1. IMAGE ANALYSIS

This technique is implied to the entire telangiectases data set. With the help of Dr. Stoecker, the parameters such as drop color value and surrounding skin size used in the design were adjusted to find all possible vessels.

2.1.1. Vessel Detection Technique. To a human, a vessel looks red compared to the surrounding skin. Using machine vision, the pixels inside the vessel have color drops from the surrounding pixels. The vessel detection technique is developed based on this fact and uses color drop with surrounding skin to find vessels. This work builds on the techniques developed by David Erdos.

In this specific application, all input images are accompanied by a lesion mask, which is a TIFF (Tagged Image File Format) image that is 0 for pixels not in the lesion, 1

for the border of the lesion and 2 for the interior of the lesion. This lesion mask is created manually with the certification from Dr. Stoecker. This algorithm iterates through every single pixel inside the lesion, selecting a new center pixel with each iteration, it then moves outward a set number of pixels (NumPix) from a given center in eight directions. It starts with the pixels labeled with the number 1 (Figure 2.2), and then the second iteration would move on to the pixels labeled with a number 2, and so on. Once a center pixel is found that matches the required color drops in two of the eight directions that are at least 135 degrees apart (e.g., North and Southwest directions are 135 degrees apart), then the center pixel is marked. According to the feature of vessels which have different color with surrounding skin, we specified different color drops for red, green and blue.

As determined experimentally, 135 degrees is large enough to compare the surrounding pixel with the center pixel; 45 degrees and 90 degrees will bring too much noise, while 180 degrees may miss some actual vessel pixels.

For example (see Figure 2.2 as a reference), starting from the North direction, assume that the first pixel in the direction of North has three values for red, green and blue color, named N_Red(1), N_Green(1) and N_Blue(1). First, we could take North and Southwest directions. Therefore,

$$((N\_Red(1) - Center\_Red > Red\_Drop \text{ and } N\_Green(1) - Center\_Green > Green\_Drop$$

and N_Blue(1) - Center_Blue > Blue_Drop) and (SW_Red(1) - Center_Red > Red_Drop and SW_Green(1) - Center_Green > Green_Drop and SW_Blue(1) - Center_Blue > Blue_Drop)) (1)

will be the one of the conditions to mark the center pixels. Besides the North and Southwest directions, the North and South directions and the North and Southeast directions should be considered as other two conditions to mask the center. It is the same for the other seven directions. When a pixel is marked, it is placed in an array that is the same size as the input image and recorded as the Boolean value of "1" [3].
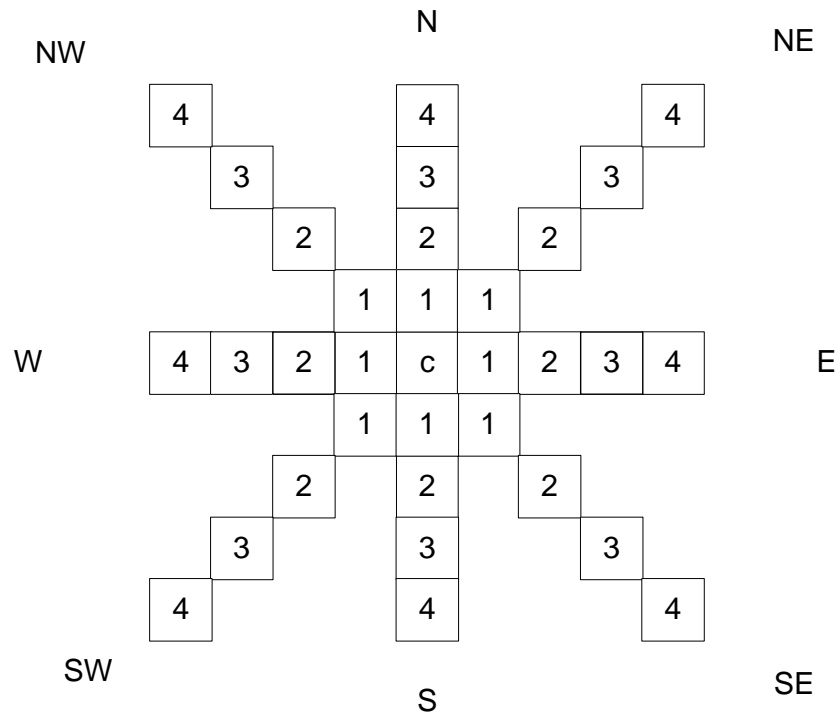

Figure 2.2: Direction Mask Used for Pixel Marking.

2.1.1.1. Drop color value.   As shown in Eq. 1, Red_Drop, Green_Drop and Blue_Drop need to be adapted to detect as many vessels as possible. By observing the color changes of the blood vessels it was determined, the red should decreaset from the

surrounding skin by more than -2 (Red_Drop) while green and blue are required to decreaset by 4 (Green_Drop) and 12 (Blue_Drop), respectively. After applying the direction mask on a pixel-by-pixel basis within the lesion and retaining the pixels that satisfy the drop constraints above, the output mask images can be obtained. Figure 2.3 presents an example of the output images based on different red color drops with 2 in (b) and -2 in (c). With decreasing the red drop from 2 to -2, some vessels missed in (b) can be detected.
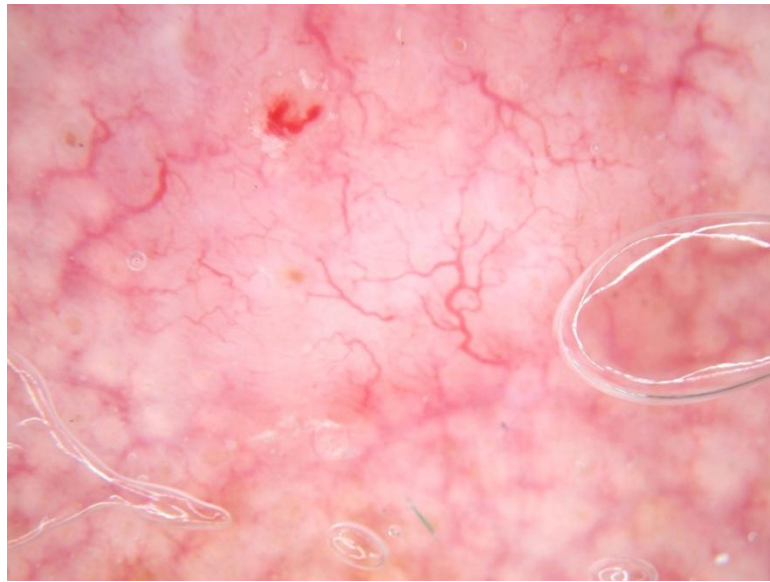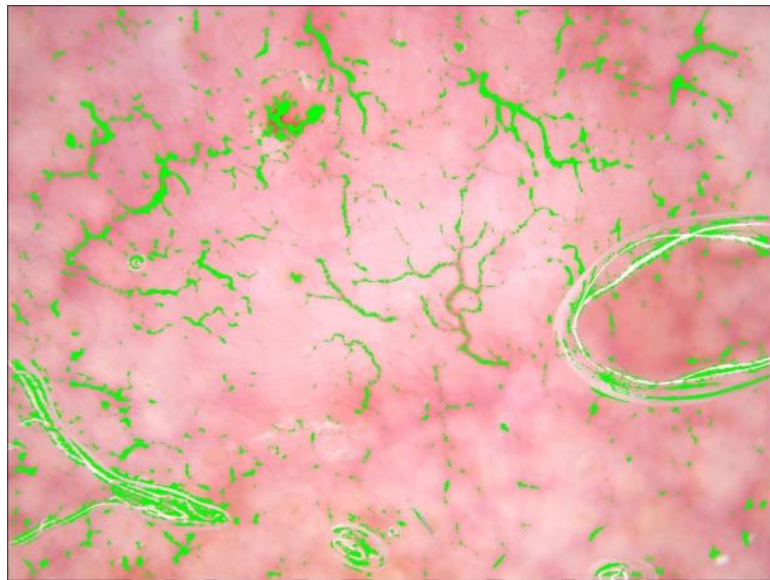

(a) Original Image

Figure 2.3: Mask Image with Different Red Drops.
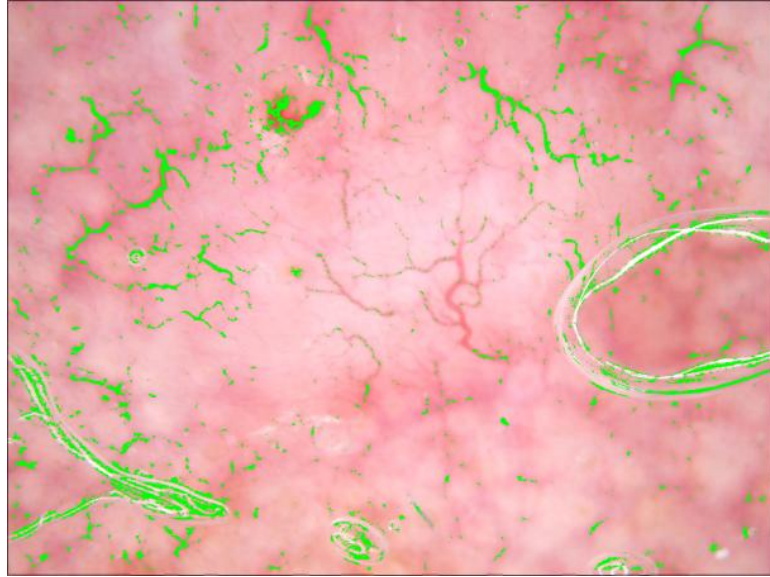
(b) Mask Image with Red Drop=2


(c) Mask Image with Red Drop=-2

Figure 2.3: Mask Image with Different Red Drops. (cont.)

2.1.1.2. Surrounding skin size. Vessels have different shapes and sizes; some are very thin while others are very thick. The thick vessels may be missed if there are not enough surrounding pixels comparing with the center one. This algorithm iterates through every single pixel inside the lesion, selecting a new center pixel with each iteration. It then moves outward a set number of pixels (NumPix) from a given center in eight directions. NumPix is the value to illustrate the surrounding skin size and has to be big enough to detect the widest vessels. Figure 2.4 shows the vessel mask using different NumPix values. Because one of the vessels in the top is very wide, it cannot be detected if NumPix is 4, but it could be found after increasing NumPix to be 7, as determined experimentally.
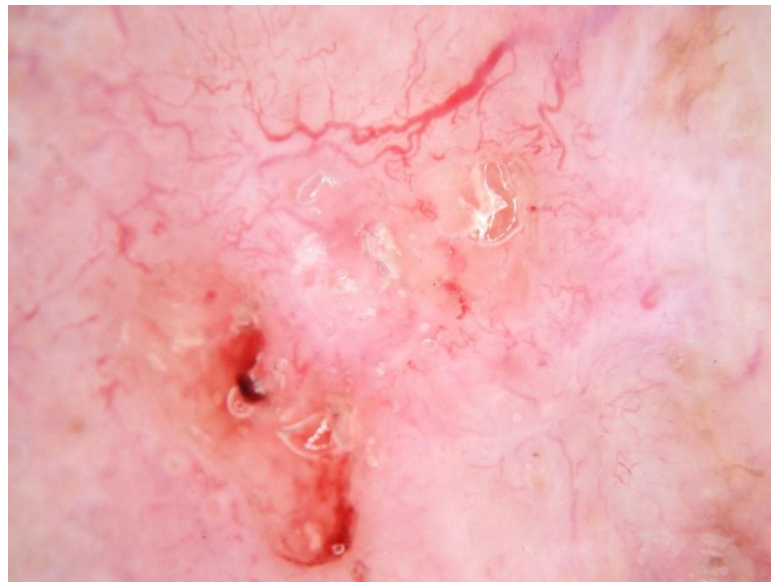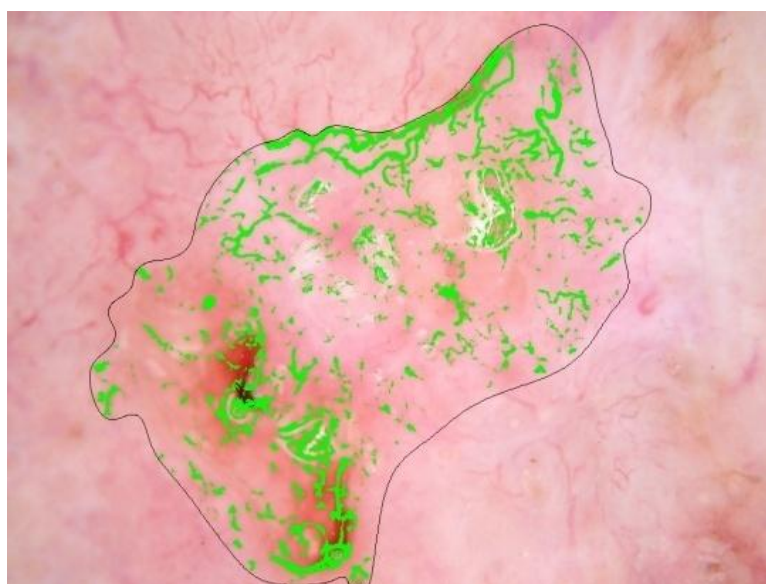

(a) Original Image

Figure 2.4: Mask Images with Different NumPix Values.
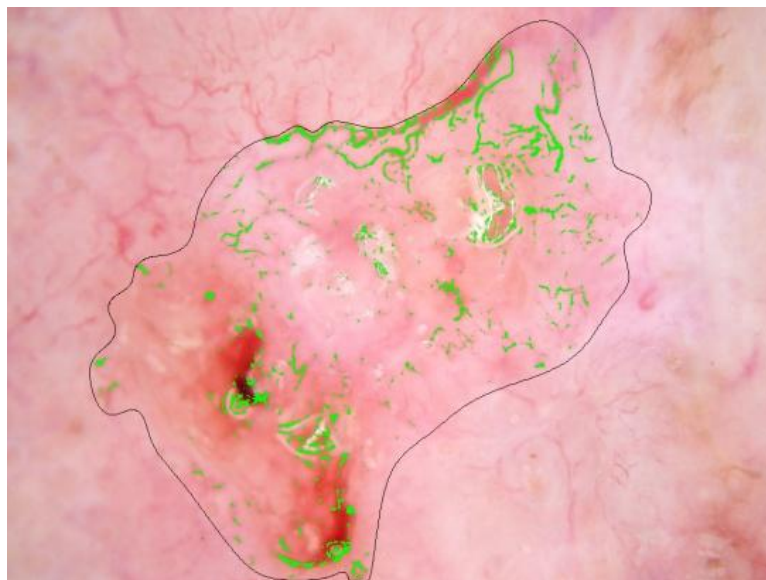
(b) NumPix=4

(c) NumPix=7

Figure 2.4: Mask Images with Different NumPix Values. (cont.)

2.1.2. Noise Filtering Technique.   After implementing the above algorithm, not only vessels, but also some other noise sources such as hair, bubble and brown area were marked. A noise filtering technique is used to mitigate these noise sources. Figure 2.5 shows brown areas that are labeled as vessels using the vessel detection technique. The following sections present noise filtering approaches used to address the different types of noise sources. All of these techniques are applied on a pixel-by-pixel basis to pixels included in the vessel mask from the vessel detection algorithm.

2.1.2.1. Brown area filtering.   For pixels within brown area structures, the green value is always bigger than the blue value. The opposite is true for vessels. This condition—Green>Blue+5, was used to filter the brown area as shown in Figure 2.6. This technique is applied on a pixel-by pixel basis to unmark the vessel mask from the vessel detection algorithm.
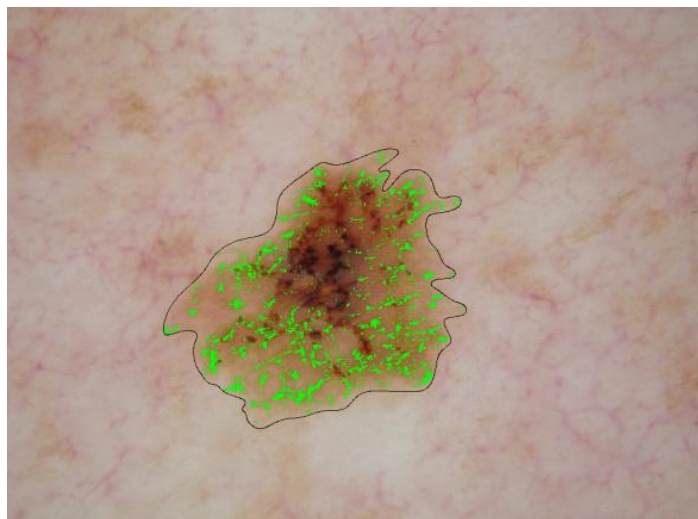

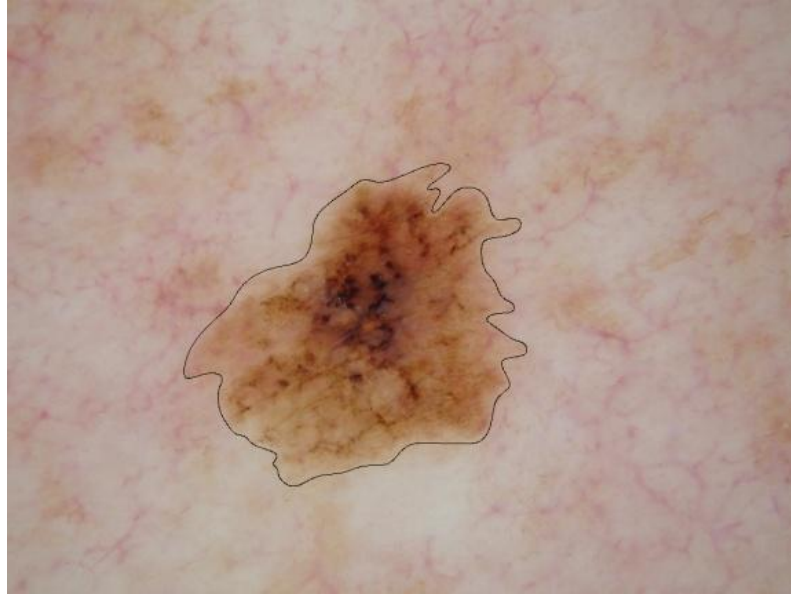Figure 2.5: Brown Area Labeled as Vessels.

Figure 2.6: Unmarked Brown Area.

2.1.2.2. Hair filtering. For skin lesions containing hair, the ratio of Red to Green has different values with the surrounding skin. We define a 5x5 square and calculate the variance of the Red/Green ratio for those 25 (5x5) pixels (Figure 2.7), then apply on a pixel-by pixel basis to unmark the vessel mask inside this square if the variance of the Red/Green ratio is greater than 0.01. The disadvantage of this algorithm is that for some wider hair or the wider part in a hair, the variance may be not greater than 0.01 so that those noise could be eliminated.
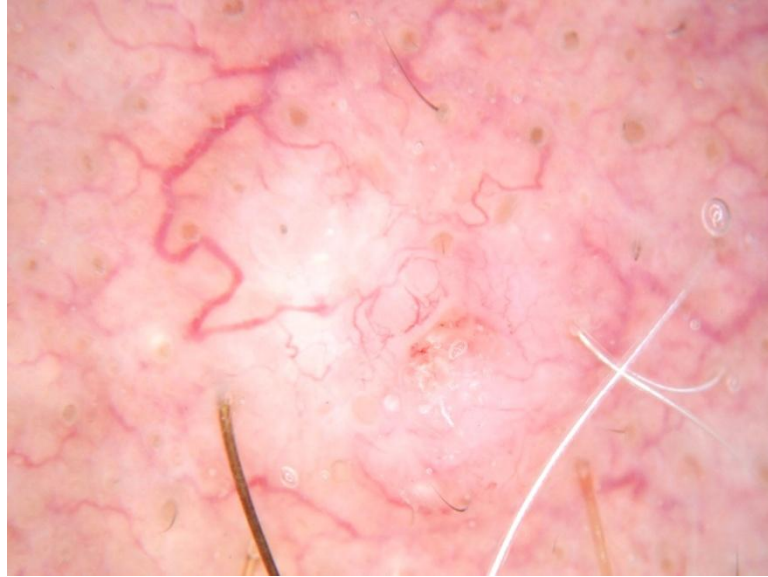
(a) Original Image
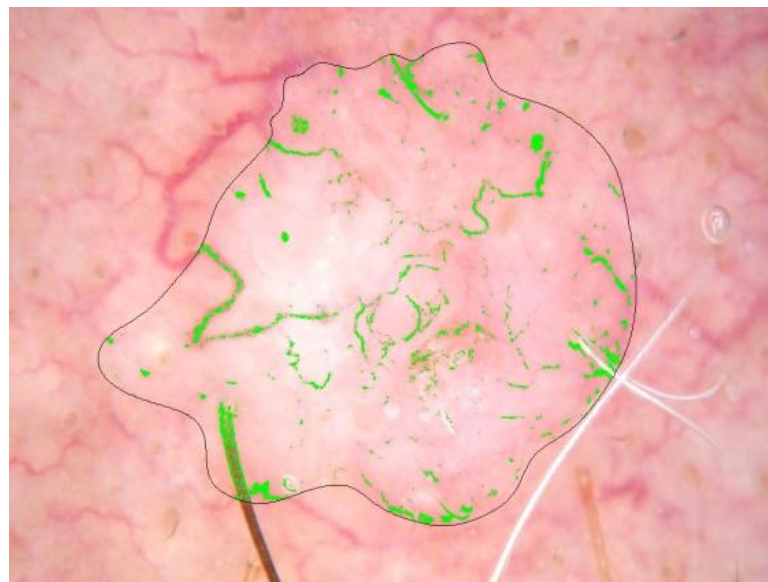
(b) Hair Labeled as Vessels

Figure 2.7: Hair Filtering.

(c) Unmarked Hair

Figure 2.7: Hair Filtering. (cont.)

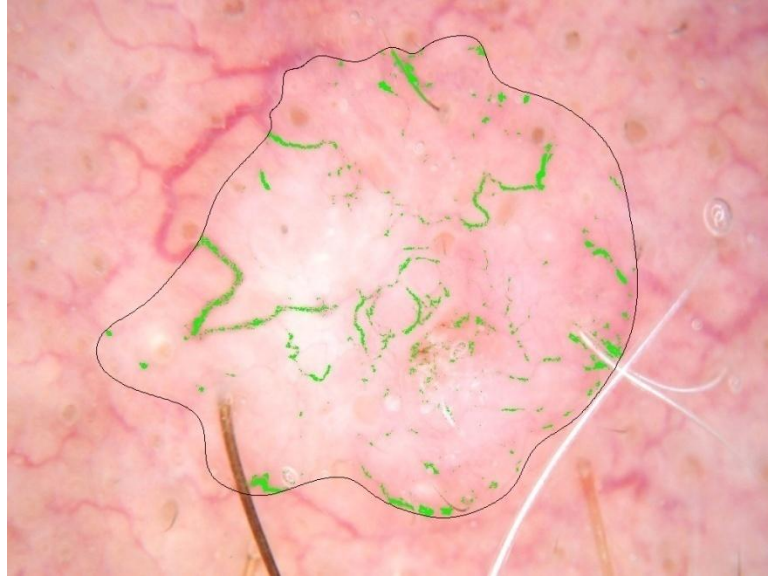**2.1.2.3. Bubble and other lighter area filtering.** Examining the image data set, there are two kinds of vessels including dark red and light red. For the light red vessels, the red color value is much larger than green value (Green/Red<0.6); for the dark red vessels, the red color value is still larger than green (Green/Red<0.7), while for bubbles and other lighter area, Green/Red has a larger ratio. Therefore, the Green/Red>0.6 constraint for light red and the Green/Red>0.7 constraint for dark red are applied on a pixel-by pixel basis to unmark the bubble and other lighter area. All of the ratio constraints were determined experimentally from the skin lesion image data set. Figure 2.8 shows an image example of filtering bubble and other lighter area.
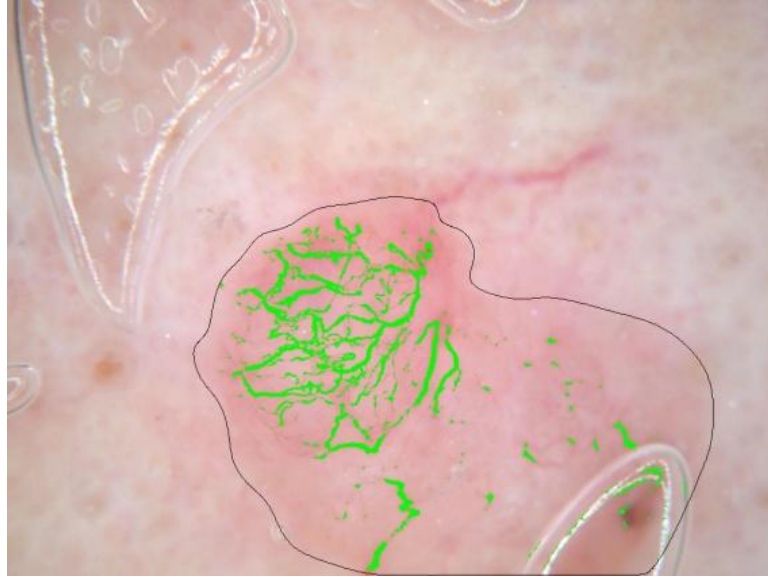
(a) Original Image

(b) Bubble Labeled as Vessels

Figure 2.8: Bubble and Other Lighter Area Filtering.

(c) Unmarked Bubble

Figure 2.8: Bubble and Other Lighter Area Filtering. (cont.)

The disadvantage of this algorithm is that although most parts of bubbles could be filtered out after this, however, some noises surrounding the bubbles are still hard to be removed.

2.1.2.4. Image dilation and erosion. Image Dilation and Erosion are used to connect the disconnected vessels. In general, a vessel should be a connected curvilinear structure, but parts of it after noise filtering become disconnected. After creating a flat, disk-shaped structuring element with radius 3, the vessel mask is dilated to see if it becomes a connected curvilinear structure. However, since the structure may become very wide after dilating, the erosion operation can be used to constrict the structure. Based on experimentation, the radius value used for the disk-shaped structuring element is 2. This technique is applied on a pixel-by-pixel basis to dilate and erode the vessel

mask for each image. Figure 2.9 shows an image example with the dilation and erosion operations applied.
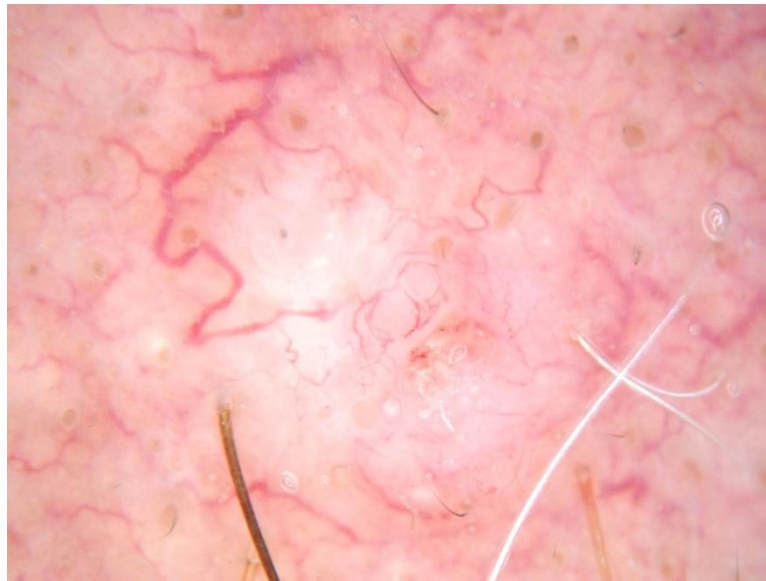
(a) Original image
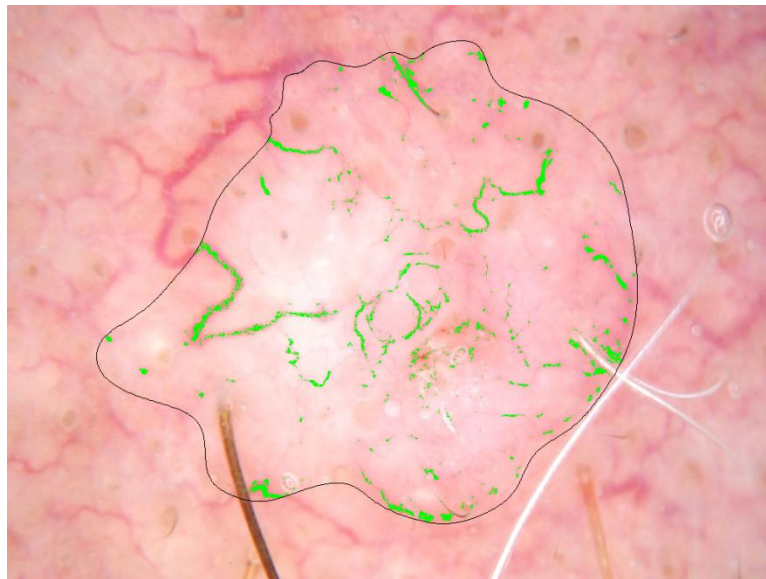
(b) Mask after Noise Filtering

Figure 2.9: Image Dilation and Erosion.
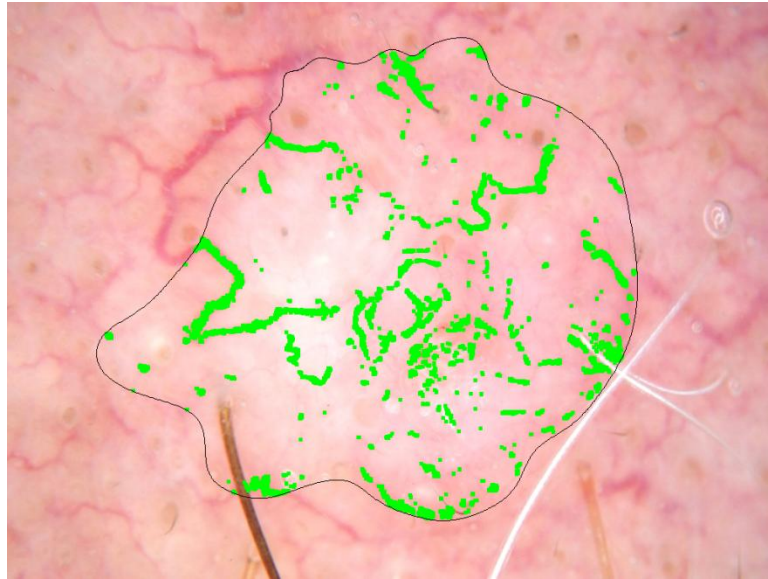
(c) Mask after Dilation (dilRad=3)
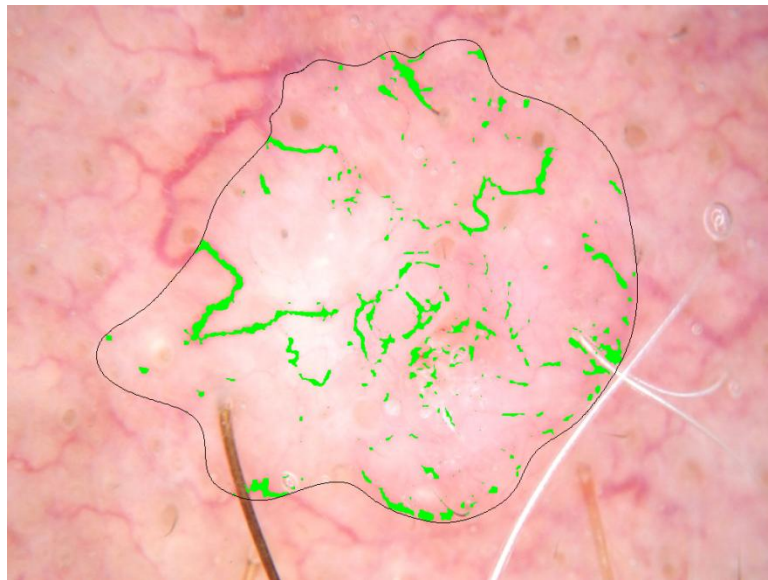
(d) Mask after Erosion (eroRad=2)

Figure 2.9: Image Dilation and Erosion. (cont.)

2.1.2.5. Square comparison algorithm. Some large blob noise could be filtered out using the square comparison algorithm. A 41x41 square is used as the standard window which is moving from the left to the right and from the top to the bottom inside the lesion for each image. If 70% or more of the pixels inside this square are marked, those pixels which were marked as vessels after the above procedure will be unmarked. As shown in Figure 2.10, the arrow in 2.10 (b) shows the big blob noise, which is filtered out in 2.10 (c).
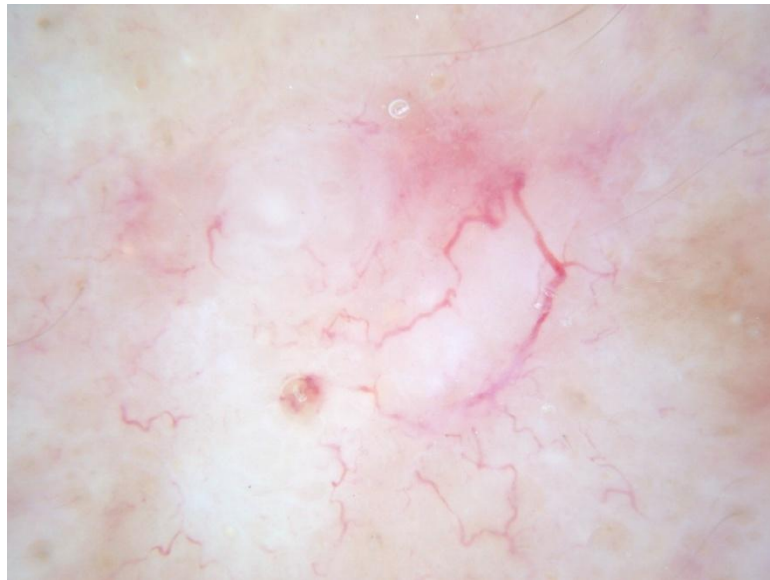
(a) Original Image

Figure 2.10: Square Comparison Algorithm.
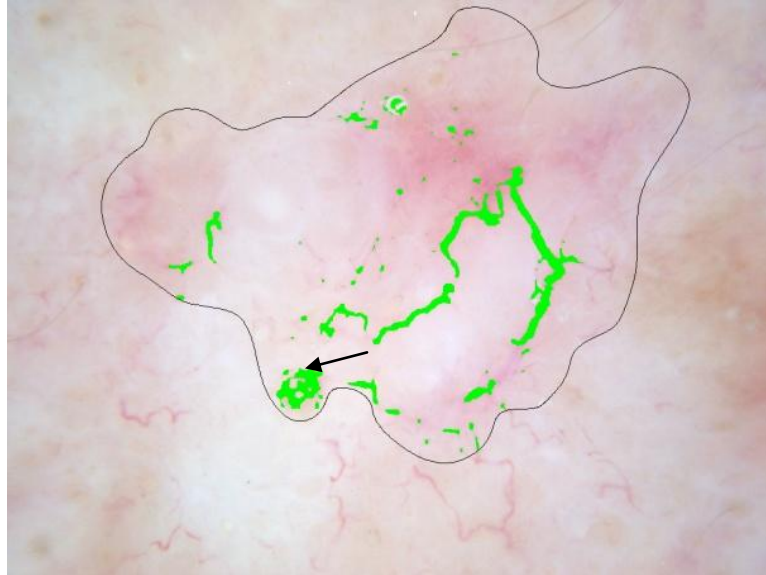
(b) Big Blob Labeled as Vessels
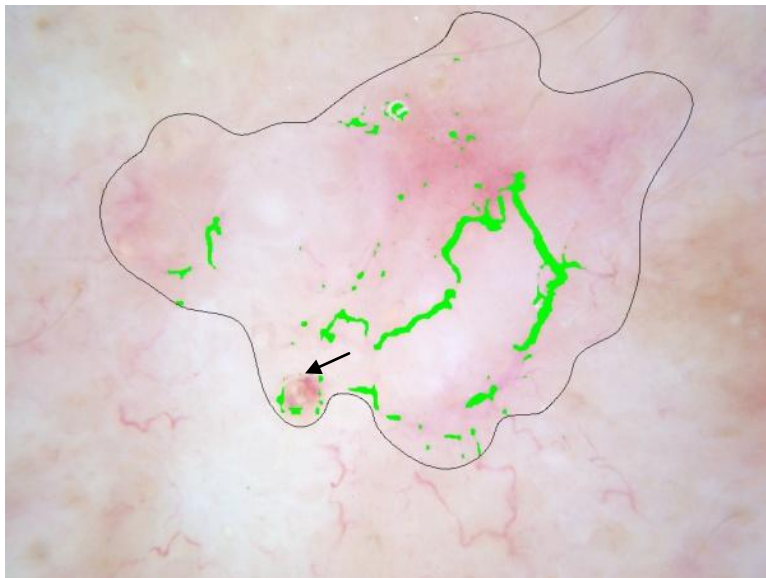
(c) Unmarked Big Blob

Figure 2.10: Square Comparison Algorithm. (cont.)

2.1.2.6. Length and area limitation. Since the result after performing all of the previous noise removal steps was still noisy and not particularly accurate, the next step is

to skeletonize the vessel mask image and remove objects that are not long enough to be considered linear vessels. For skeletonization, the Matlab® function bwmorph(BW, 'skel') executed to perform skeletonization. This operation is used to remove pixels on the boundaries of objects but does not allow objects to break apart and the pixels remaining make up the image skeleton. The minimum object length of the skeleton is defined as 30 pixels. Any object will be removed if its length is less than the required value. In addition to applying the skeleton length constraint for object removal, objects with an area of less than 40 pixels are eliminated as too small. Figure 2.11 presents an image example with the skeletonization length and object area constraints applied. Figure 2.11 (a)-(d) give the original image, vessel mask after applying the vessel detection and noise removal algorithms described in Section 2.1.2.5, vessel mask with length constraint applied and vessel mask with area constraint applied, respectively.
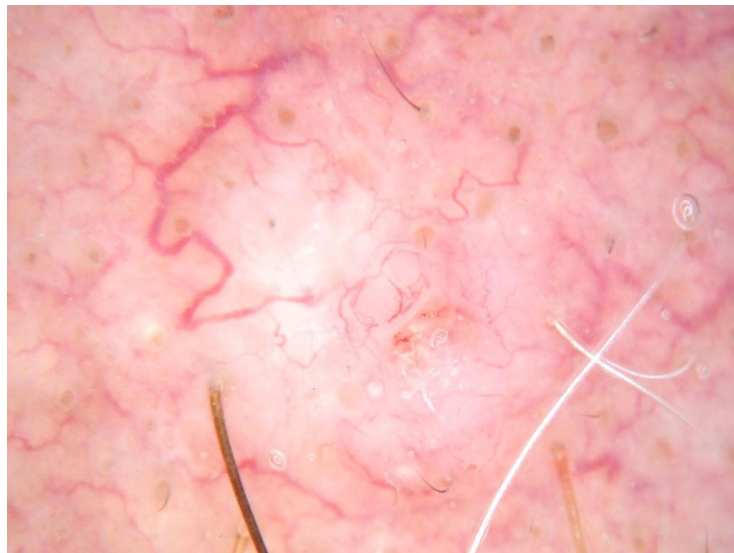
(a) Original Image

Figure 2.11: Length and Area Limitation.
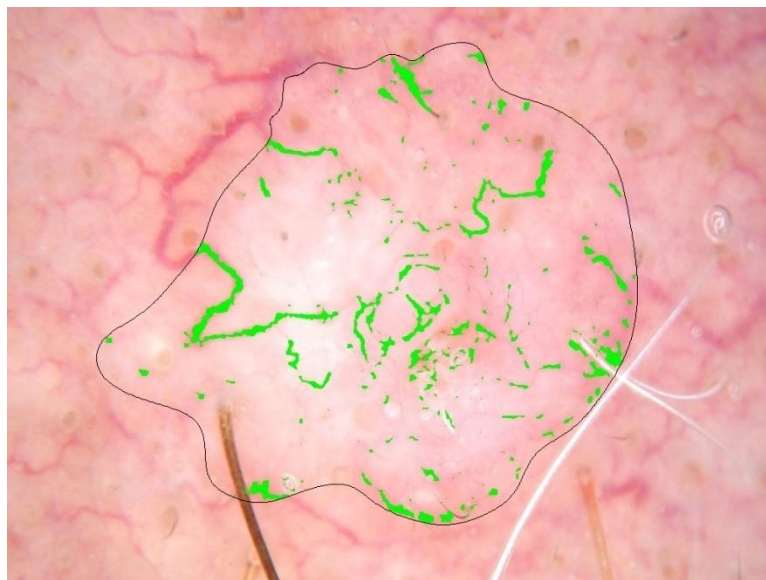
(b) Mask with Noise
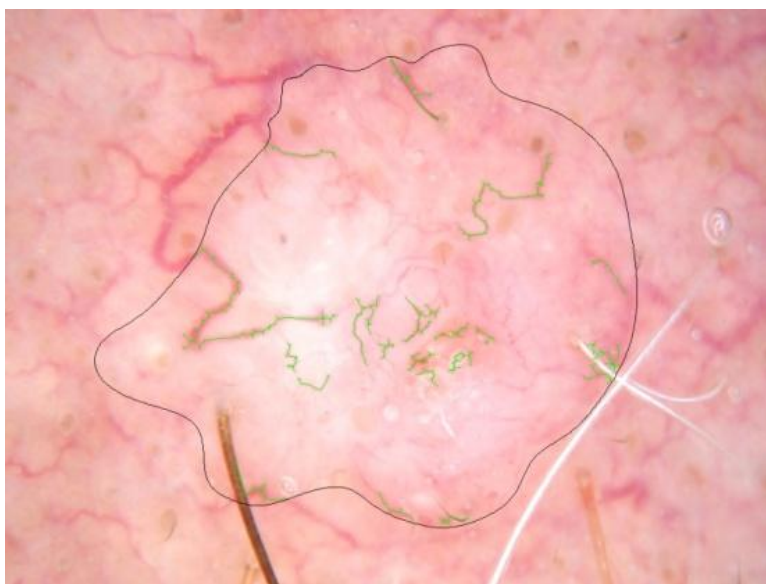
(c) Mask after Length Limitation

Figure 2.11: Length and Area Limitation. (cont.)
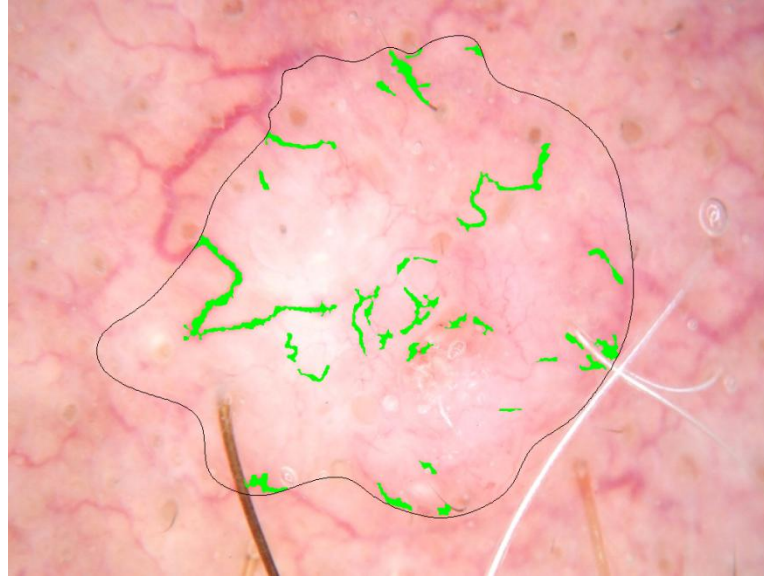
(d) Mask after Area Limitation

Figure 2.11: Length and Area Limitation. (cont.)

2.1.3. Contrast and Brightness Change. For some telangiectases images, which have low contrast and there are few vessels detected after implementing the above algorithm, a contrast enhancement technique can be applied. For this reason, the contrast and brightness need to be adjusted to find more vessels. Working with dermatologist, Dr. Stoecker, the parameters of brightness and contrast need were determined to be -68 and +27, respectively, as determined from three images of the data set using Paint.net [http://www.paint.net]. These brightness and contrast values were applied to all images in the data set using the brightness and contrast function in Adobe Photoshop®. The original image and the image with brightness decrease and contrast enhancement are shown in Figure 2.12.

(a) Original Image

(b) Image After Brightness and Contrast Change

Figure 2.12: Different Images Before and After Changing Brightness and Contrast.

Also, the original telangiectases mask and the telangiectases mask after changing

Brightness and Contrast are shown in Figure 2.13.

(a) Telangiectases Mask Before Brightness and Contrast Change
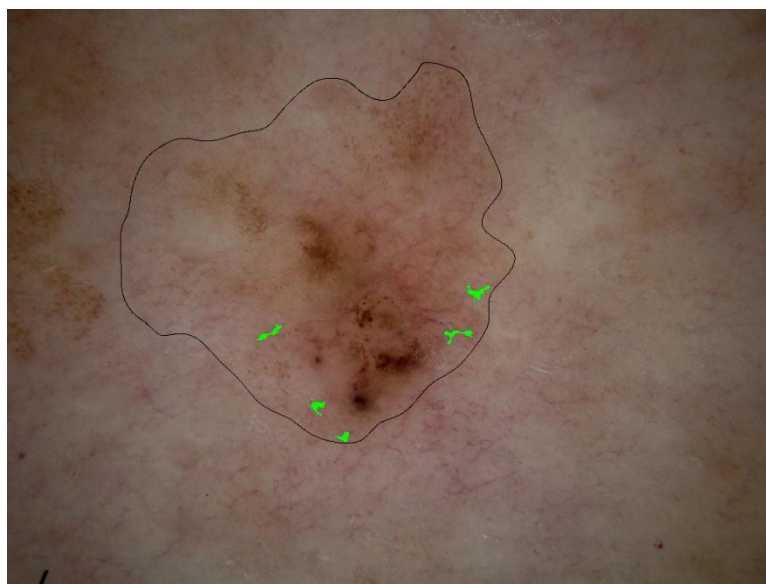
(b) Telangiectases Mask After Brightness and Contrast change

Figure 2.13: Different Masks Before and After Changing Brightness and Contrast.

However, for some benign competitive images, the vessel masks contain an increasing number of false vessels after changing the contrast and brightness in the color

images. Figure 2.14 shows the original image and the image with brightness decrease and contrast enhancement. Figure 2.15 shows this example with the original mask and the mask after changing brightness and contrast.

(a) Original Image

(b) Image After Brightness and Contrast Change

Figure 2.14: Different Images Before and After Changing Brightness and Contrast.
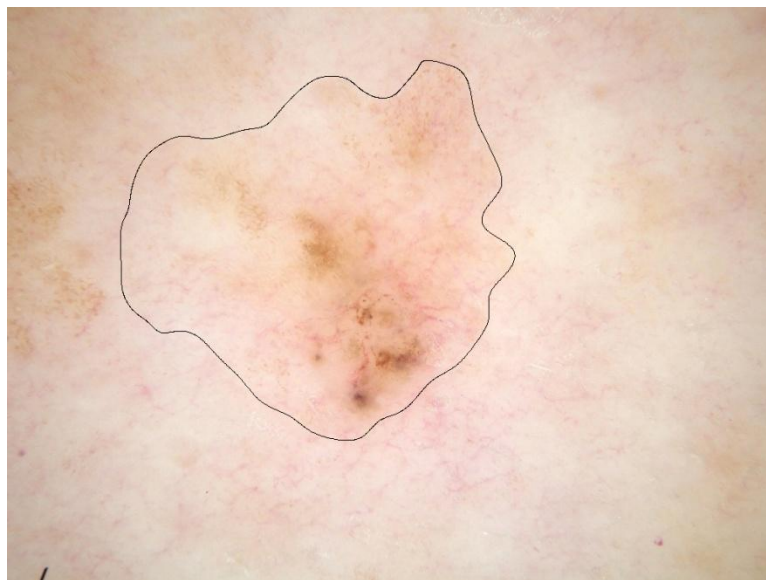
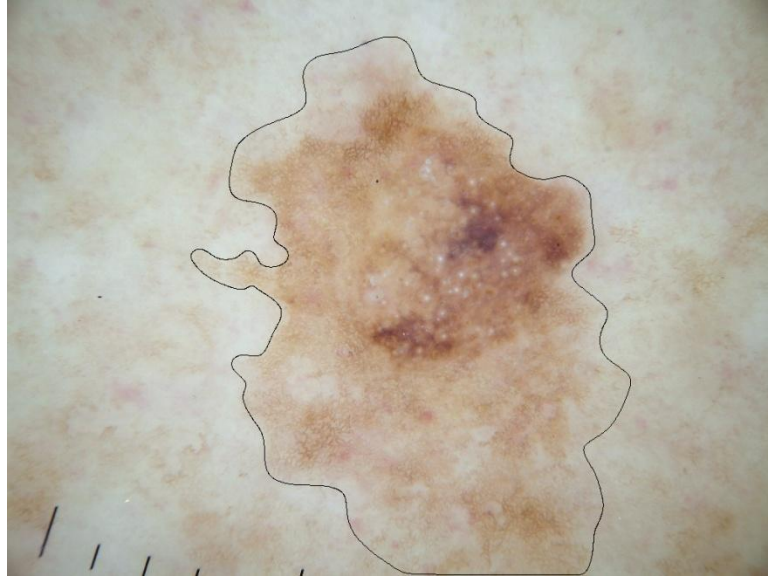(a) Mask Before Brightness and Contrast Change
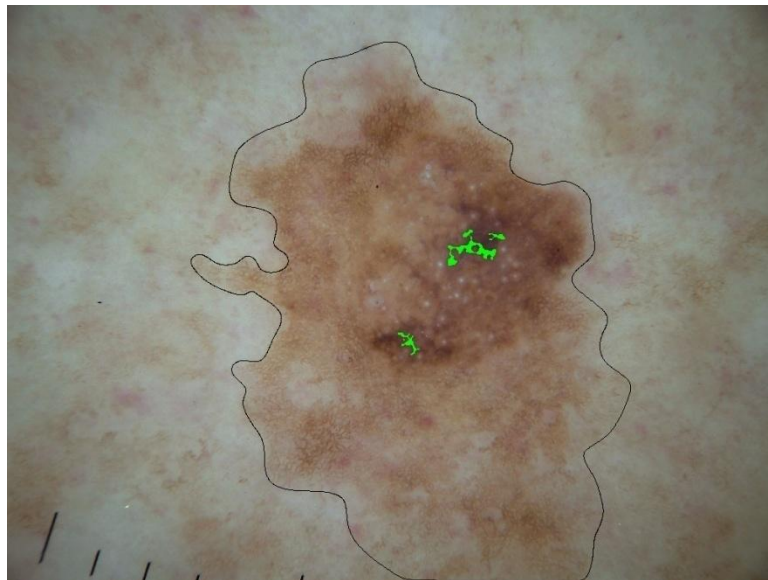
(b) Mask After Brightness and Contrast Change

Figure 2.15: Different Masks Before and After Changing Brightness and Contrast.

Therefore, to balance the tradeoff between using all original images and using all contrast and brightness changed images, a conditional contrast enhancement is

implemented. The contrast value is determined by calculating the standard deviation of all the pixels inside the lesion area for each image. If this value is less than the threshold , which is set up as 14.47 by experiment, the responsible contrast and brightness changed image should be used; otherwise, the original image is used as the input. For this research, only conditional contrast enhancement images are used for the feature generation for lesion discrimination.

2.2. FEATURE GENERATION

The final vessel mask is generated after applying the algorithm with noise removal steps presented in Section 2.1. For this research, there were 59 telangiectases and 235 no-telangiectases dermoscopy images for analysis. The telangiectases images are of lesions that have been diagnosed with Basal Cell Carcinoma (BCC). The no-telangiectases images are of benign lesions. However, in some non-telangiectases images, part of them are still marked as the telangiectases in the final mask. To discriminate telangiectases from normal vessels characteristic of a benign lesion, the following features were computed from the final vessel mask:

- *Object number/Lesion area.* This represents the ratio of the total number of telangiectases objects to the lesion area. Benign dermoscopy images usually have a lower value of object number/lesion area ratio than telangiectases images.

- *Maximum Object length after skeletonizing/sqrt(Lesion area).* It represents the ratio of maximum length among the entire telangiectases objects to square root of the lesion area after skeletonizing. Benign dermoscopy images usually have a lower value.

- *Maximum Object area/lesion area*. This represents the ratio of maximum area among all the telangiectases objects before skeletonization to the lesion area. Benign dermoscopy images usually have a lower value.

- *Average Object length after skeletonizing/sqrt(Lesion area)*. This represents the ratio of average length among all the telangiectases objects after skeletonization and square root of the lesion area. Benign dermoscopy images usually have a lower value.

- *Average Object area/ sqrt(Lesion area)*. This represents the ratio of average area among all the telangiectases objects before skeletonizing and square root of the lesion area. Benign dermoscopy images usually have a lower value.

- *Average width of all objects/sqrt(Lesion area)*. For telangiectases, the width of each object should not be too large, while, it is possible for the vessels in benign lesions to have a greater width.

- *Standard Deviation width of all objects/sqrt(Lesion area)*. For benign images, standard Deviation width of all objects/sqrt(Lesion area) could be greater.

- *Maximum Eccentricity*. The eccentricity is the ratio of the distance between the foci of the ellipse enclosing the candidate vessel and its major axis length. Benign images may have a greater value.

- *Average Eccentricity*. Benign images may have a greater value.

- *Object Number within ten Erosions*. Erode the Telangiectases mask with the radius from 1 to 10 and record the remaining object number for each erosion.

- *Area within ten Erosions*. Erode the Telangiectases mask with the radius from 1 to 10 and record the remaining mask area for each erosion.

2.3. LESION DISCRIMINATION

In order to evaluate the effectiveness of the vessel detection process, lesion discrimination is performed using the two classes Basal Cell Carcinoma (BCC) and benign lesions. Two approaches for lesion discrimination are investigated, including a multilayer perceptron back propagation neural network and particle swarm optimization (PSO) using a neural network. These approaches are presented as follows.

2.3.1. MLP Back Propagation Neural Network [4]. Three different MLP back propagation neural Networks are created according to different input features. All neural networks are implemented in Matlab®.

For the first work, the input is the total 30 features. The 30 features computed over the image data set include *Object number/Lesion area*, *Maximum Object length after skeletonizing/Lesion area*, *Maximum Object area/lesion area*, *Average Object length after skeletonizing/Lesion area, Average Object area/Lesion area, Average width of all objects/Lesion area, Standard Deviation width of all objects/Lesion area, Maximum Eccentricity, Average Eccentricity, Object Number within ten erosions (10 Features), Area within ten erosions (10 Features).* So for this neural network, the neural network architecture is 30x18x10x1, with 29 features and a bias in the input layer, 18 nodes in the first hidden layer, 10 nodes in the second hidden layer and one output. Sigmoid transfer functions are used in the input and hidden layers, and a linear transfer function is used in the output layer.

For the second work, the input is 19 features. The 19 features computed over the image data set include *Object number/Lesion area*, *Maximum Object length after skeletonizing/Lesion area*, *Maximum Object area/lesion area*, *Average Object length*

after skeletonizing/Lesion area, Average Object area/Lesion area, Average width of all objects/Lesion area, Standard Deviation width of all objects/Lesion area, Maximum Eccentricity, Average Eccentricity, Object Number within ten erosions (10 Features). The neural network architecture is 20x4x2x1.

For the third work, the input is the 19 features including *Object number/Lesion area*, *Maximum Object length after skeletonizing/Lesion area*, *Maximum Object area/lesion area*, *Average Object length after skeletonizing/Lesion area*, *Average Object area/Lesion area*, *Average width of all objects/Lesion area*, *Standard Deviation width of all objects/Lesion area*, *Maximum Eccentricity, Average Eccentricity, and Area within ten erosions (10 Features)*, The neural network architecture is 20x4x2x1.

Because of the relatively small data set, a leave-one-out methodology is used for training/test set generation for all neural network architectures. The neural networks are trained up to 15 epochs or until root-mean-square error was less than 0.001.

There are two kinds of MLP Back Propagation Neural Network training---online training and offline learning. In online (Stochastic/Delta) learning, the weights are adjusted after each pattern presentation. In this case, the next input pattern is selected randomly from the training set, to prevent any bias that may occur due to the sequences in which patterns occur in the training set. In offline (batch) learning, the weight changes are accumulated and used to adjust weights only after all training patterns have been presented. Online Training is used in this project, which means that the weights are updated after each pattern is presented. The target value for the telangiectases data set (class 1) is set to be 1 and for the competitive benign data set (class 0) to be 0. The result

after testing are not the binary values 0 and 1, some outputs are between 0 and 1 and some of them even have negative values.

Receiver operating characteristic (ROC) curve are generated for classification results based on the neural network outputs obtained for the leave-one-out cases. A ROC curve is a graphical plot of the sensitivity for a binary classifier system as its discrimination threshold is varied. The ROC can also be represented equivalently by plotting the fraction of true positives (TP = true positive rate) versus the false negative rate (FN = false negative rate).

Figure 2.16 shows the plot of ROC curves and areas under the ROC CURVES for the neural network results based on the three different feature combinations. All neural network results presented are based on on-line neural network training. For the different ROC curves presented, the vertical axis shows the true positive rate, and the horizontal axis gives the false negative rate.
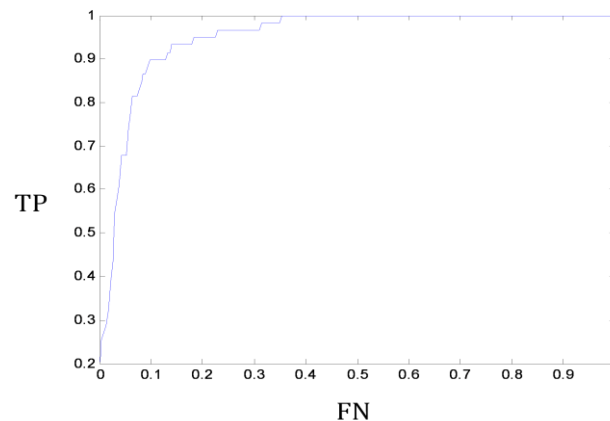
(a) ROC Curve for the First 10 Features and 10 Area Features: Area= 0.952

Figure 2.16: ROC Curve for Different Neural Network Architectures.
TP=True Positive Rate; FN=False Negative Rate.
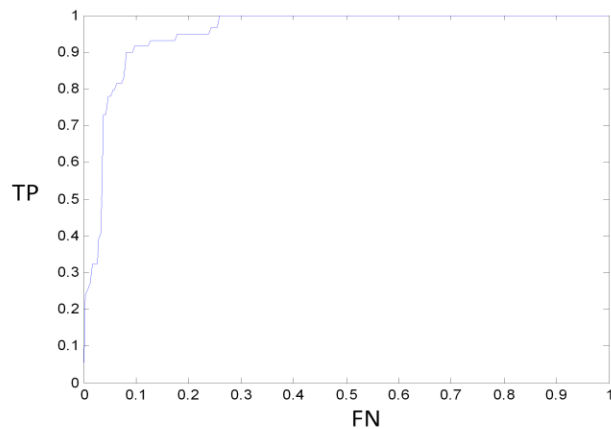
(b) ROC Curve for the First 10 Features and 10 Object Features: Area= 0.959

(c) ROC Curve for First 10 features, 10 Area Aeatures, 10 Object Features: Area=0.94

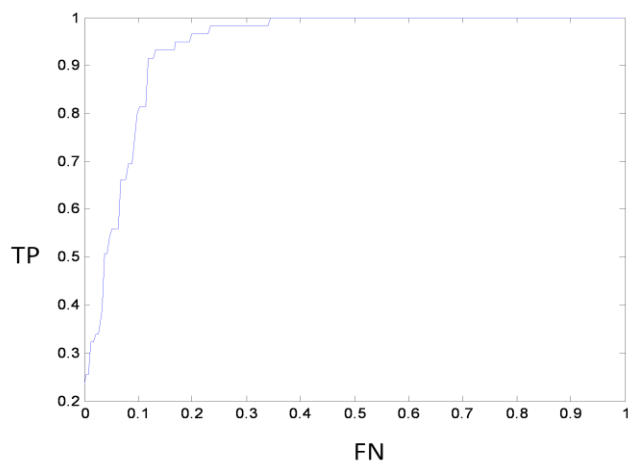Figure 2.16: ROC Curve for Different Neural Network Architectures. TP=True Positive Rate; FN=False Negative Rate. (cont.)

2.3.2. Particle Swarm Optimization. Stochastic optimization approach is modeled on the social behavior of bird flocks and/or fish school. The ability of birds to fly synchronously and to suddenly change direction and regroup in an optimal formation is used as the original model for Particle Swarm Optimization [5]. Each bird inside the flocks could be considered as a particle. Each particle represents a candidate solution to the optimization problem and is 'flown' toward the possible direction. A particle adjusts its position according to its own experience and the experience of neighboring particles.

In this algorithm, each particle has random velocity and memory that keeps track of previous best position and corresponding fitness. The previous best value of the particle position is called the 'pbest'. It has another value called 'gbest', which is the best value of all the 'pbest' positions in the swarm. The basic concept of PSO is that each particle in the swarm move toward its pbest and gbest locations at each time step. (Figure 2.17)
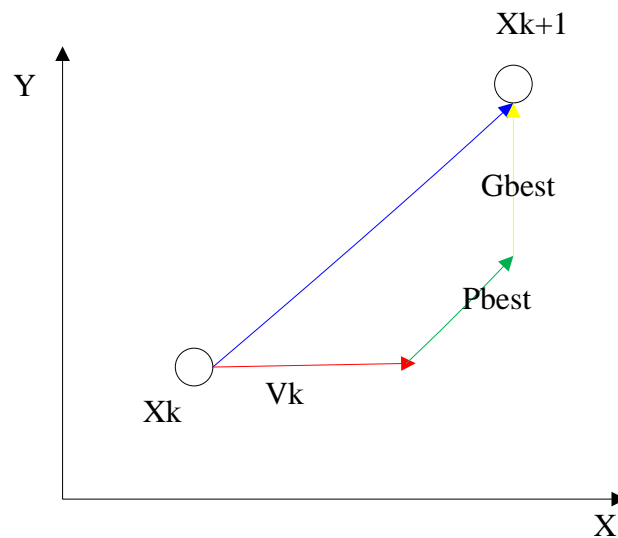
Figure 2.17: Basic Concept of PSO.

The velocity of the particles is given as follows:

$$V_{id}(k + 1) = wV_{id}(k) + c_1 rand_1\big(Pbest_{id} - X_{id}(k)\big) + c_2 rand_2\big(Gbest_{id} - X_{id}(k)\big) \tag{2}$$

The position vector of the particles is changed as follows:

$$X_{id}(k + 1) = X_{id}(k) + V_{id}(k + 1) \tag{3}$$

Where,

k – Current iteration (time step)

i – Current particle

d - Dimension

$V_{id}(k)$ – Particle's current velocity

$V_{id}(k + 1)$– Particle's new velocity

$X_{id}(k)$– Particle's current position

$X_{id}(k + 1)$– Particle's new position

w – Inertia weight

c_1 – Cognitive acceleration constant

c_2 – Social acceleration constant

Pbest – Particle's overall best position

Gbest – Best position of the swarm

$rand_1$ And $rand_2$ – random numbers from a uniform distribution, U (0, 1).

2.3.2.1. MLP neural network trained by PSO. In this research, PSO is used to train a MLP neural network. The procedure is provided below.

Step1: initialize particle set, P, with initial weight value from W and V vectors.

Step2: go through the feed-forward equations. Then use the MSE of each particle solution as the fitness of each particle and to update the Gbest and Pbest values.

Step3: the PSO velocity and position equations will update the new weight changes for each particle.

Step4: if the error is less than the Target error, terminate the program. Otherwise, go to Step2.

2.3.2.2. MLP neural network architecture. In this neural network, the input is the first 9 features including *Object number/Lesion area, Maximum Object length after skeletonizing/Lesion area, Maximum Object area/lesion area, Average Object length after skeletonizing/Lesion area, Average Object area/Lesion area, Average width of all objects/Lesion area, Standard Deviation width of all objects/Lesion area, Maximum Eccentricity, Average Eccentricity*. Let x denote the feature vector computed for each image from the final vessel mask, therefore, the network has 10 linear neurons in the input layer (input 'x' along with bias value of 1), 5 (unipolar) sigmoid neurons in the hidden layer and 1 linear neuron in the output layer. The target value for melanoma (class 1) is set to be 1 and for non-melanoma (class 0) is set to be 0.

Both the training data set and the testing data set have to be normalized before implementing as the input for neural network. The mean and standard deviation are obtained for each feature from the training set of feature vectors, then each data set is normalized by the equation:

$$(x - mean(X))/std(X) \tag{4}$$

Offline (batch) learning is used in this PSO-based implementation, which means that the weight changes are accumulated and used to adjust weights only after all training patterns have been presented. Both telangiectases and no-telangiectases data sets are divided into ten subsets as shown in Figure 2.18.

Therefore, for telangiectases, each subset almost has 5 images while for no-telangiectases, each subset almost has 23 images. Nine subsets from the telangiectases data set and nine subsets from the no-telangiectases data set are taken as the training data set while the remaining subset from each is taken as the testing data set. For example, firstly, subset 2~10 from both data sets are taken as the training set while subset 1 is used as the testing set. Secondly, subsets 1 and 3~10 would be taken as the training set while subset 2 is the testing set and so on. Therefore, each time there are 54 telangiectases and 212 no-telangiectases images for training and five telangiectases and 23 no-telangiectases images for testing. See Figure 2.19. After 10 times, each subset is tested and an ROC curve area can be generated.
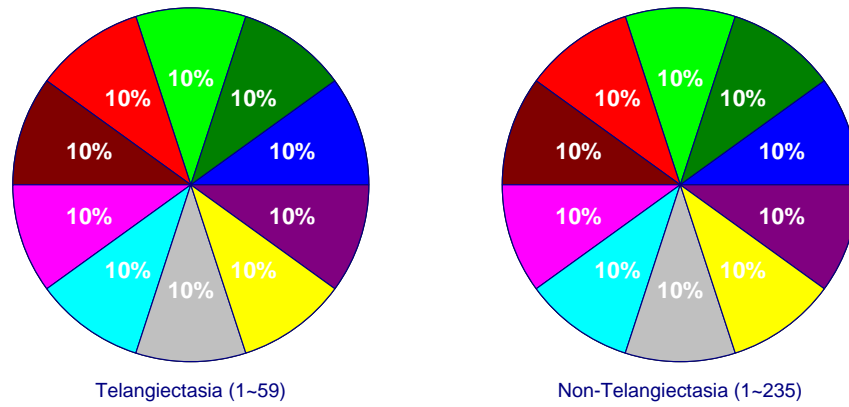
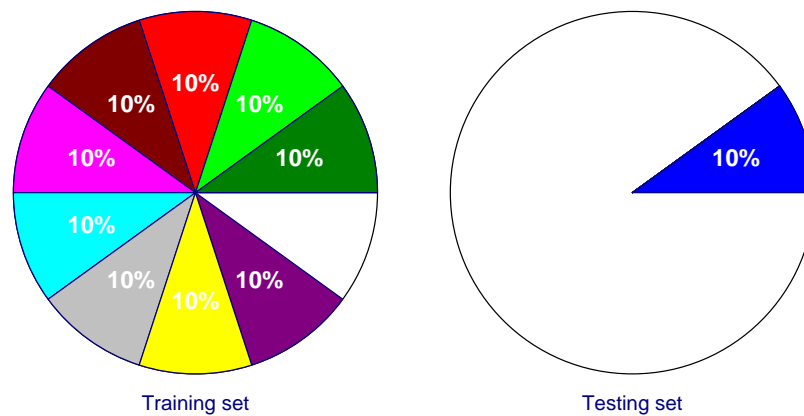Figure 2.18: Ten Subsets for Each Data Set.

Figure 2.19: Diagram of 90% as Training and 10% as Testing.

Based on applying the PSO neural network-based algorithm to the ten training/test sets, the area under the ROC Curve for each training/test set is 0.861, 0.904, 0.861, 0.957, 0.939, 0.957, 0.861, 0.868, 0.951 and 0.868. Therefore, the average ROC curve area is 0.9027.

3. RESULTS AND DISCUSSION

The ROC curve area result of different neural network algorithms are presented and compared in this part. Table 3.1 shows the ROC curve area result for from the first to the tenth training/test set and the average ROC curve area result using the PSO neural network-based Algorithm. Table 3.2 shows the ROC curve area result for the MLP back propagation neural network algorithm using different features.

Generally, the MLP Neural Network trained by Backpropagation gives better result than PSO neural network-based algorithm. The reason for this is that the leave-one-out methodology is used for Backpropagation Algorithm while PSO neural network-based algorithm uses ten percent data for testing and ninety percent data for training. Based on the fact that a relatively small data set is generated in this research, the more data that is applied in training, the higher the accuracy that is obtained.

For the comparison of the three structures of MLP Backpropagation neural networks, the 19 features including *Object number/Lesion area*, *Maximum Object length after skeletonizing/Lesion area*, *Maximum Object area/lesion area*, *Average Object length after skeletonizing/Lesion area, Average Object area/Lesion area, Average width of all objects/Lesion area, Standard Deviation width of all objects/Lesion area, Maximum Eccentricity, Average Eccentricity, Object Number within ten erosions (10 Features)* give the best result. The reason is probably due to the object number within ten erosions in benign lesion images has a more distinguished decrease than BCC images. The area within ten erosions does not play such a good role.

Figure 3.1 shows one of the BCC images which is discriminated as a benign lesion falsely. The vessel is not long enough to be considered as telangiectases. Figure 3.2 shows one of the benign lesion images which is discriminated as BCC falsely. The noise around the bubbles and the noise around the hair could not be removed after applying the noise filter technique. Those areas are long and big enough to be considered as telangiectases.

Table 3.1: ROC Curve Area Result for PSO-Based Algorithm.

Training Set Number	Test Set Number	Area under ROC Curve
2~10	1	0.861
1, 3~10	2	0.904
1~2, 4~10	3	0.861
1~3, 5~10	4	0.957
1~4, 6~10	5	0.939
1~5, 7~10	6	0.957
1~6, 8~10	7	0.861
1~7, 9~10	8	0.868
1~8,10	9	0.951
1~9	10	0.868
Average Area under ROC Curve		0.903

Table 3.2: ROC Curve Area Result for Backpropagation Algorithm.

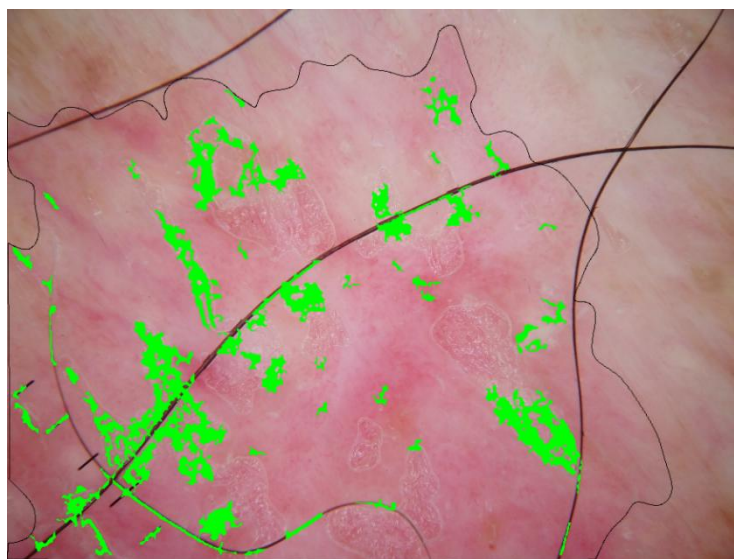|	
ROC curve for the first 10 features and 10 area features	0.952
ROC curve for the first 10 features and 10 object features	0.959
ROC curve for first 10 features, 10 area features, 10 object features	0.940

(a) Original Image

(b) Telangiectases Mask

Figure 3.1: Falsely Discriminated BCC Image.

(a) Original Image

(b) Telangiectases Mask

Figure 3.2: Falsely Discriminated Benign Lesion Image.

4. CONCLUSION AND FUTURE SCOPE

Essentially this research investigated an approach to find vessel-type structures in dermoscopy skin lesion images based on applying color drop and noise removal image processing techniques and performing classification basal cell carcinoma/benign skin lesion discrimination based on computational intelligence algorithms. For the first component, based on the fact that some of images are fuzzy, the contrast enhancement technique could be added to increase the contrast. Therefore, the conditional contrast enhancement technique is implemented firstly. After applying this, the vessel detection technique is used and noise filter technique is added to remove noise from the mask. For the second component, two computational intelligence algorithms, including MLP back propagation neural network and MLP neural network trained by PSO, are presented and compared to discriminate basal cell carcinoma from benign lesions based on features computed for skin lesions with normal vessels from lesions containing telangiectases. Experimental results have shown that MLP back propagation neural network gives a better outcome than the PSO-based approach.

Although the current discrimination accuracy is fairly high, there is some improvement needed for the future scope of this work. The parameters used in the contrast enhancement technique affect the output images in a manner that results in different vessel masks. Therefore, a new research method, Adaptive Critic Design, could be used to increase the ROC curve area by inputting the features extracted from the mask images with different levels of contrast enhancement. In the future work, ACD would be implemented instead of MLP back propagation neural network or the PSO-based method.

BIBLIOGRAPHY

[1]   Jean L. Bolognia, Dermatology, pp.1653-1654, 2406. New York: Mosby, 2003.

[2]   R. J. Stanley, R. H. Moss, W.V. Stoecker, C. Agarwal, "A fuzzy based histogram analysis technique for skin lesion discrimination in dermatology clinical images," CMIG, vol. 27, no. 5, pp. 387-396, 2003.

[3]   David Erdos, "Telangiectases detection in dermoscopy images," OURE Report, University of Missouri-Rolla, 2007.

[4]   Y. Hirose, K Yamashita, and S Hijiya. "Back-Propagation Algorithm Which Varies the Number of Hidden Units," Neural Networks, vol. 4, pp. 61-66, 1991.

[5]   J. Kennedy and R. C. Eberhart, "Particle swarm optimization," Proc. 1995 IEEE International Conference on Neural Networks, Nov. 27-Dec. 1, 1995, Piscataway, NJ, USA, vol.4,pp.1942-19

VITA

Beibei Cheng was born on Dec 30, 1984 in Anhui Province, China. She received her Bachelor of Science degree in Electronics Engineering in 2005 from University of Electronic Science and Technology of China. She received her Masters degree in Computer Engineering from Missouri University of Science and Technology in 2009.